NTHAS7: The Seventh Korea-Japan Symposium on Nuclear Thermal Hydraulics and Safety
Chuncheon, Korea, November 14- 17, 2010

N7P0032

NUMERICAL STUDY OF THREE DIMENSIONAL THERMAL HYDRAULICS EFFECT ON THERMAL STRATIFICATION PHENOMENA IN UPPER PLENUM OF MONJU

Takuji Sakamoto[1*], Makoto Shibahara[1], Takashi Takata[1] and Akira Yamaguchi[1]

[1] Graduate School of Engineering, Osaka University
2-1 Yamadaoka, Suita, Osaka, Japan, 565-0871
+81-6-6879-7895 , sakamoto_t@qe.see.eng.osaka-u.ac.jp

ABSTRACT

Thermal stratification phenomena will take place at an upper plenum of liquid metal fast breeder reactor (LMFBR) when a reactor trip operation is initiated. Since the thermal stratification gives rise to thermal stress on the upper plenum structure, it is of importance to investigate the characteristics of the phenomena.

In the present study, a three dimensional numerical investigation of the stratification has been carried out using a commercial CFD code, FLUENT. The trip test from 40% power output condition in Monju, prototype fast breeder reactor in Japan, is chosen as the benchmark problem.

In the analyses, a parametric study has been done with a simplified configuration. Furthermore, a comparatively fine mesh arrangement has been applied for the comparison of the experimental result. As a result, the behavior of the thermal stratification interface is well demonstrated by using fine mesh from the trip to 240s after the trip. Furthermore, it has been demonstrated that the high temperature coolant at the upper side of the plenum plays as a plug at certain duration from the beginning by calculating the temperature distribution and the stream regime in the entire upper plenum finely. Hence, the outflow to the exit of the upper plenum (hot leg pipes) goes mainly through small holes (flow holes) that are placed at the inner barrel in Monju.

1. INTRODUCTION

When a reactor trip operation is initiated in a liquid metal fast breeder reactor (LMFBR), a low temperature coolant is fed through the core outlet to the bottom side of the upper plenum of the reactor. Consequently, thermal stratification phenomena will be observed at the upper plenum because a higher temperature coolant remains at the beginning of the trip. A thermal stratification gives rise to thermal stress on structural components in the upper plenum. Therefore, it is important to investigate characteristics of the phenomena and to evaluate the magnitude of the thermal stress.

In order to investigate the behavior of the thermal stratification, many numerical studies were conducted as well as various scaled model experiments using water or liquid sodium as a working fluid (Ieda et al., 1990). In Japanese Prototype Fast Breeder Reactor "Monju", a turbine trip test from 40% power output conditions was conducted in 1995 (Doi et al., 1996). In the test, the thermal stratification phenomenon was observed by measuring the temperature distribution at the upper plenum. Recently, a detailed engineering data of the test was summarized as a benchmark problem of the International Atomic Energy Agency (IAEA) (Yoshikawa et al., 2009).

A multi-dimensional thermal hydraulic simulation is one of the best ways to investigate the stratification phenomena especially when liquid sodium is used as a working fluid. Concerning with the Monju turbine trip test, several thermal hydraulic analyses were conducted, such as to understand the stratification process (Doi et al., 1997) and to investigate the stratification phenomenon at trip from 100% power output operation (Suda et al., 2002).

However, a comparatively coarse mesh arrangement was applied in the previous works so that empirical correlations such as a pressure drop coefficient were required in the analysis. From the viewpoint of the extension of the test result from 40% to 100% power output operation condition, it is desirable that those empirical correlations are solved directly in the numerical simulation.

In the present study, a three dimensional numerical investigations have been carried out without implementing the empirical correlation of the pressure drop coefficient. A commercial CFD code, FLUENT ver.6.3.26 is used for the simulation.

In the analyses, a parametric study of the mesh arrangement and the time step size has been conducted firstly. Then the benchmark analyses of the Monju turbine trip test have been carried out.

2. MONJU TURBINE TRIP TEST

Monju is a loop type LMFBR and liquid sodium is used as a coolant. Figure 1 shows the schematic of the Monju cooling pipe system. It consists of the primary, the secondary, and the water/steam heat transport systems.

In the test, 40% power output was set as an initial condition and the turbine trip was conducted manually. After the trip, the circulation pump of the primary heat transport system stopped immediately and a pony motor was activated. As a result, the flow rate of the primary coolant decreased by following the characteristics and was kept to be 10% of the rated operation. At the same time, the pump stop and the activation of the pony motor was also operated in the secondary system Furthermore, the circulation of the secondary system changed to the air cooler system (ACS) from the steam generator (SG).

Figure 2 shows the geometry of the upper plenum. It consist of the Upper Core Structure (UCS), TC-plug, core barrel, outlet nozzles, fuel handling machine, dip plate, reactor nozzle, fuel transfer machine lower guide, in-vessel racks, inner barrel and honeycomb structure including SATCs and flow guide. The axial temperature in the upper plenum was measured with TC-plug. Upper flow holes and lower flow holes are the holes bored in the inner barrel. The coolant passes through those flow holes and the flow pattern of coolant is very complicated.

Figures 3(a) and 3(b) show the typical flow rate and temperature of the channel at the core outlet under the transient condition (Doi et al., 1996). As shown in these figures, the flow rate and temperature of the channel decrease gradually as the time passes.

Figure 4 shows the typical temperature distribution after trip measured by Yoshikawa (Yoshikawa et al., 2009). It can be seen from this figure that thermal stratification interface was observed between lower flow holes and top of inner barrel during 600s.

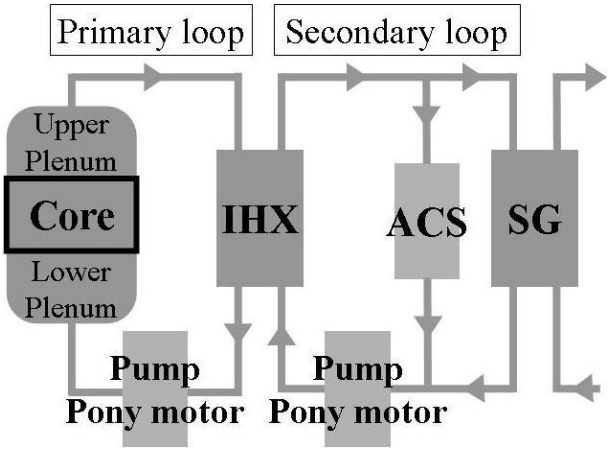

Fig. 1 The heat transport system in Monju

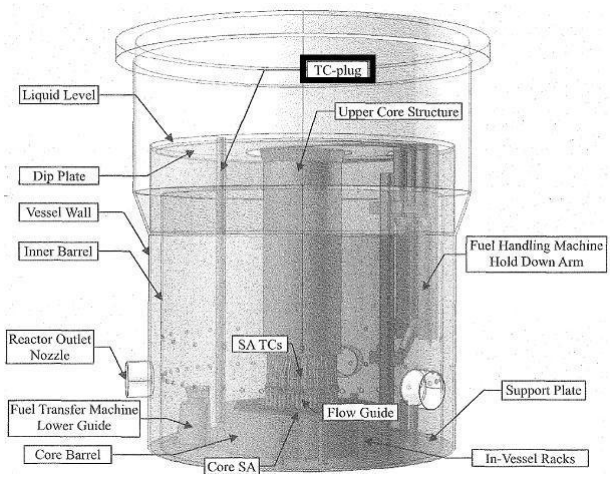

Fig. 2 Geometry of the upper plenum in Monju

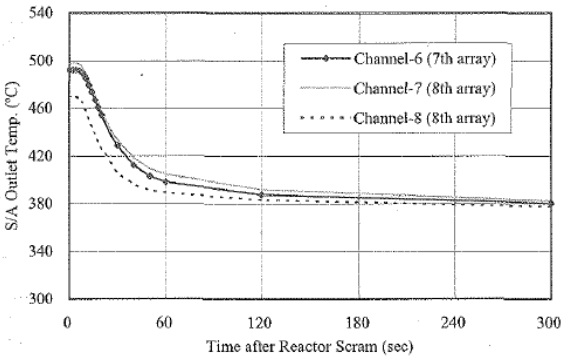

(a) Flow rate

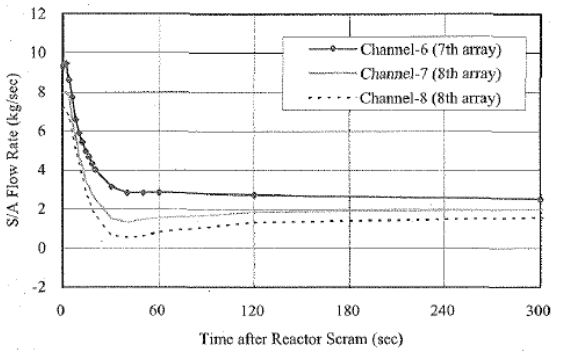

(b) Temperature

Fig. 3 Flow rate (a) and temperature (b) at the core outlet

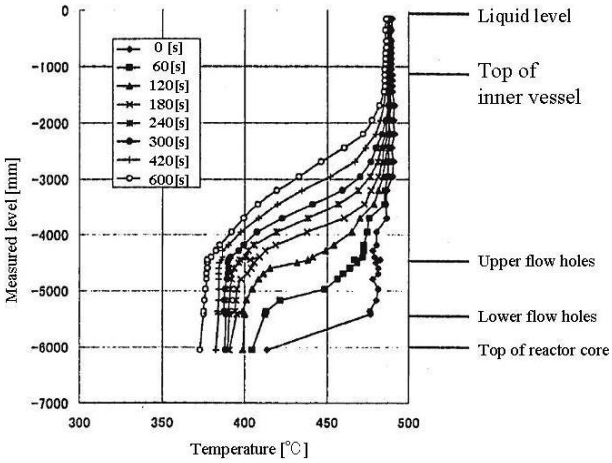

Fig. 4 Experimental temperature distribution axial direction during 600s

3. NUMERICAL ANALYSES

The parametric study and benchmark analysis were conducted under the steady and transient conditions. In the parametric study, the effects of mesh arrangement and time step size were investigated. As mentioned in the introduction, the thermal stratification interface was influenced by the pressure drop coefficient at the flow hole which is given as the slit configuration (Doi et al., 1997). However, it is important to understand the flow ratio of flow hole to annulus region in the upper plenum, when the thermal stratification interface rises with the increase of cold sodium. In order to evaluate the flow rate of flow hole, we focused on the mesh arrangement at the flow hole using unstructured grid to clarify the effect of the configuration of flow hole. Based on the parametric study, the benchmark analysis was performed under the IAEA benchmark condition.

3.1 Parametric study

3.1.1 Analytical condition

Figure 5 shows the analytical model of the upper plenum. The upper plenum consists of upper core structure, TC-plug, core barrel, inlet nozzle, outlet nozzle, inner barrel, and flow holes. The shape of the flow holes is circle.

The reactor structures such as the honey comb structure and fuel handling machine were simplified. Also, the number of the channel at the core outlet is reduced from 19 channels to 6 channels. This simplification is allowed because the results of this parametric study are compared not with the results of experiment but with the results of each other.

Figure 6(a) and 6(b) show the mesh arrangement. In order to evaluate the flow rate at the flow hole, finer meshes in the flow holes were arranged as shown in Fig.6(b). The numbers of meshes generated by Gambit 2.4.6 were about 457,000 meshes for CaseP1 and 2,172,000 meshes for CaseP2. The sizes of the meshes around the flow holes are about 0.02m for CaseP1 and about 0.01m for CaseP2, respectively.

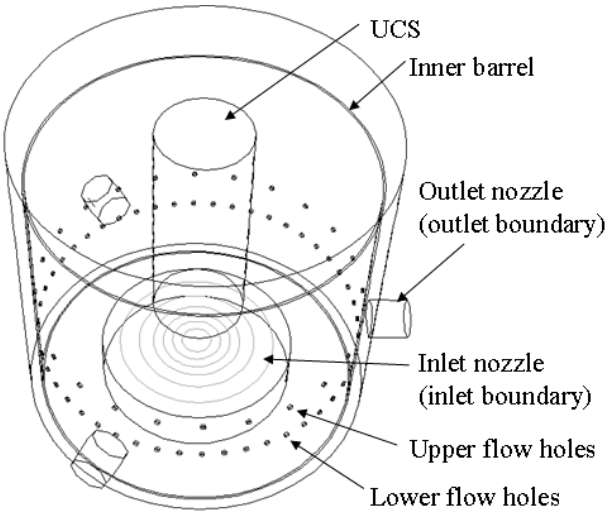

Fig. 5 Analytical model of the upper plenum for the parametric study

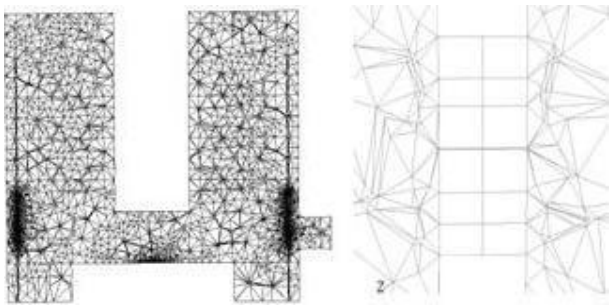

Vertical cross-sectional view, flow hole

(a) CaseP1

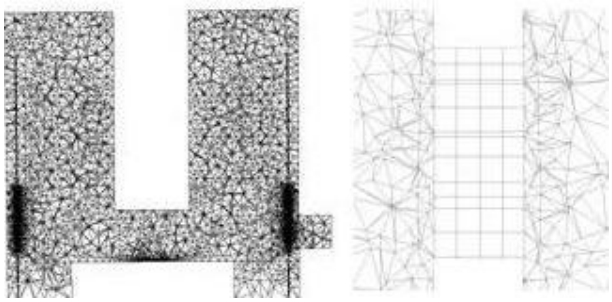

Vertical cross-sectional view, flow hole

(b) CaseP2

Fig. 6 Cross-sectional view of mesh arrangement

3.1.2 Boundary conditions and numerical method

As the flow rate and the sodium temperature at the inlet boundary, the data of the flow rate and the sodium temperature measured at 900s were used which were based on the IAEA benchmark condition (Yoshikawa et al., 2009). The physical properties of coolant are defined with polynomial, which depend on the sodium temperature. Since the buoyancy force would work for the stratified flow, the effect of gravity was considered. The reactor structures such as upper core structure, core outlet, outlet nozzles, and inner barrel were adiabatic condition.

The basic conservation equations were discretized using Finite Volume Method (FVM) in FLUENT code ver. 6.3. In this numerical analysis, standard k-ε model (SKE) was used for CaseP1 and CaseP2. In this numerical analysis, the convective term and time marching term were calculated the first order upwind scheme.

3.1.3 Results and discussion

Figures 7(a) and 7(b) show the axial temperature distribution during 600s. As shown in these figures, the thermal stratification was observed between flow holes and top of inner barrel. It was understood that the temperature at the flow holes decreases due to mixing with cold sodium, which flows in the upper plenum after trip. Also, it can be seen from this figure that the thermal stratification interface rise was pushed up by cold sodium during 600s. And then, for comparison between CaseP1 and CaseP2, it was understood that the mesh arrangement around the flow hole influences on

the behavior of thermal stratification.

On the other hand, the effect of time step on the thermal stratification was indicated in Fig. 8. This figure shows the axial temperature distribution at 600s. As show in this figure, it was confirmed that the behavior of the thermal stratification in this analytical model was scarcely influenced by the time step. Consequently, the fine mesh arrangement and the time step of 2s will be used for the following the benchmark analysis.

Figure 9 shows the mass flow rate of the annulus region, the upper flow holes (F/H) and the lower flow holes during 600s. It can be seen from this figure that the mass flow fraction of the flow holes increases as the mass flow fraction of the annulus region decrease. It was considered that the temperature at the flow holes was influenced by the mass flow fraction of the flow holes to the fraction of the annulus region. Thus, the position of thermal stratification interface depended on the mass flow ratio of flow holes to the fraction of the annulus region. The remarkable difference was not found between CaseP1 and CaseP2.

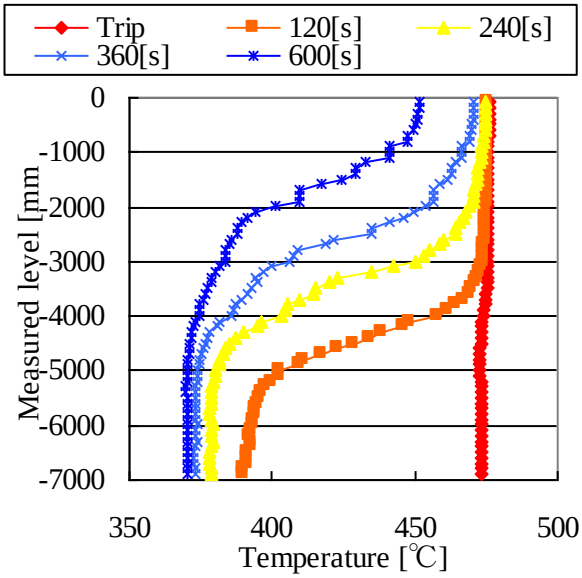

(a) CaseP1

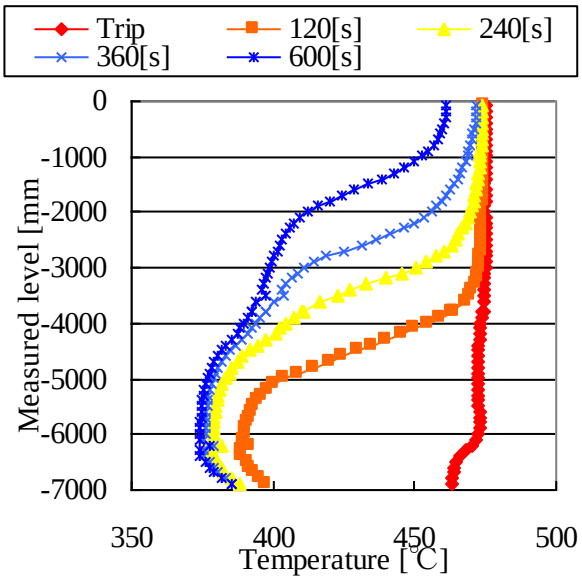

(b) CaseP2

Fig. 7 Axial temperature distribution after trip

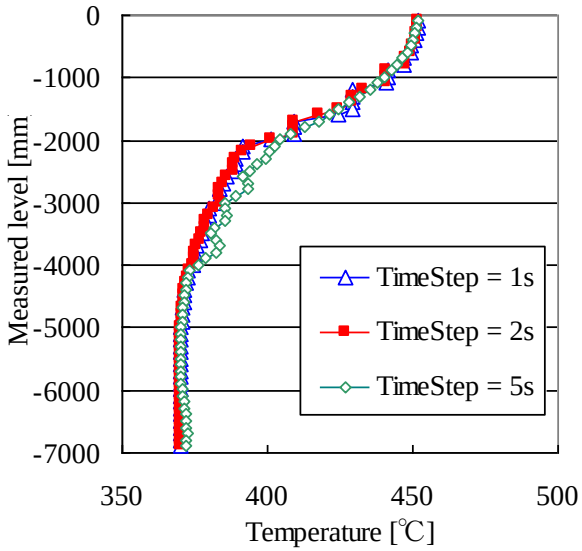

Fig. 8 Axial temperature distribution at 600s

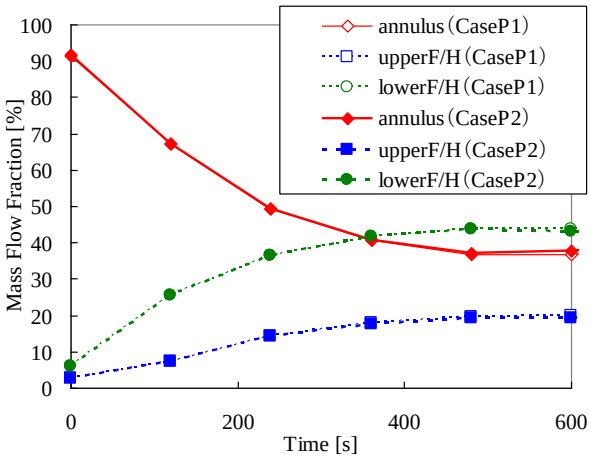

Fig. 9 The flow ratio of the flow holes to the annulus region

3.2 Benchmark analyses

3.2.1 Analytical condition

Figure 10 shows the analytical model for benchmark analyses. The upper plenum is consisted of upper core structure, TC-plug, core barrel, H/L pips, fuel handling machine and inner barrel. The honey comb structure at the core outlet and flow guide tubes between the upper core structure and the core outlet is taken into account the porous media body with the porosity of 0.5. In this analysis, the numbers of meshes were 510,000. Figure 11 shows the mesh arrangement in the vertical cross-sectional view. The sizes of the meshes around the flow holes are about 0.01m which is based on the knowledge acquired in the parametric analysis.

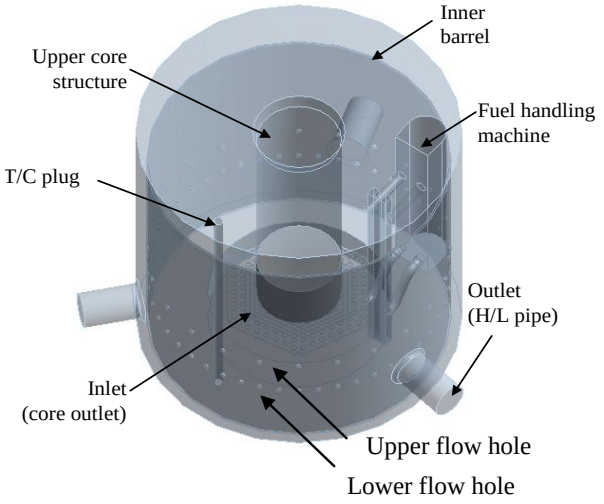

Fig. 10 Schema of the upper plenum

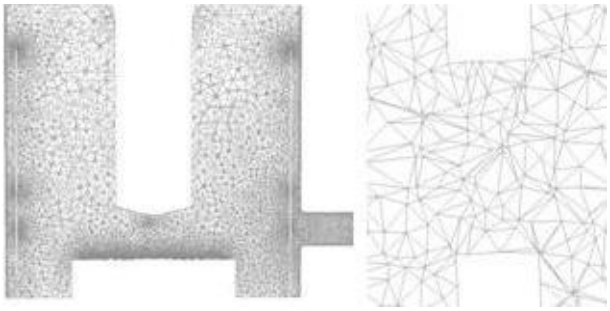

Vertical cross-sectional view, flow hole

Fig. 11 Cross-sectional view of meshes

3.2.2 Boundary condition and numerical method

The flow rate and the sodium temperature at the core outlet were based on the IAEA benchmark condition (Yoshikawa et al., 2009). The reactor structures such as fuel handing machine, upper core structure, core outlet, outlet nozzles, TC-plug, and inner barrel were adiabatic condition.

The basic conservation equations were discretized using Finite Volume Method (FVM) in FLUENT code ver. 12.0. FLUENT ver. 12.0. was used because the quality of analysis was improved from FLUENT ver.6.3. In this numerical analysis, the convective term was calculated using QUICK scheme is applied to convective terms so as to reduce a numerical diffusion (Maekawa, 1990) and the time marching term is calculated by the second order Euler implicit method. The time step size is set to 2s based on the parametric study. The standard k-ε model is used as a turbulence model and the SIMPLE algorithm is used as a numerical solution.

3.2.3 Results and discussion

Figure 12 shows the comparison of the axial temperature distribution between the analysis and the test at the TC-plug (see Fig. 10). The symbols show the experimental data for the reactor trip under the 40% power (Doi et. al. 1996) while the lines with symbols show the numerical results under the IAEA benchmark condition.

At the initial condition, a quite good agreement is achieved except the bottom of the TC-plug (lower than -6000mm) as shown in Fig. 12. The bottom side of the analytical region lower than the core outlet is assumed as an adiabatic wall in the simulation. On the contrary, a bypass flow exists at the bottom boundary in the actual plant which temperature is as same as that in the lower plenum. Hence the underestimation of the temperature is investigated in the analysis.

After trip, the interface of the thermal stratification rises gradually as the cold sodium flows to the upper plenum. As shown in Fig.12, the sodium temperature of numerical solution agrees with the experimental data at an early stage of the transient (0-240s). However, the cold temperature region seems to develop rapidly in the analysis rather than in the experiment after 240s and thus the elevation of the interface is overestimated.

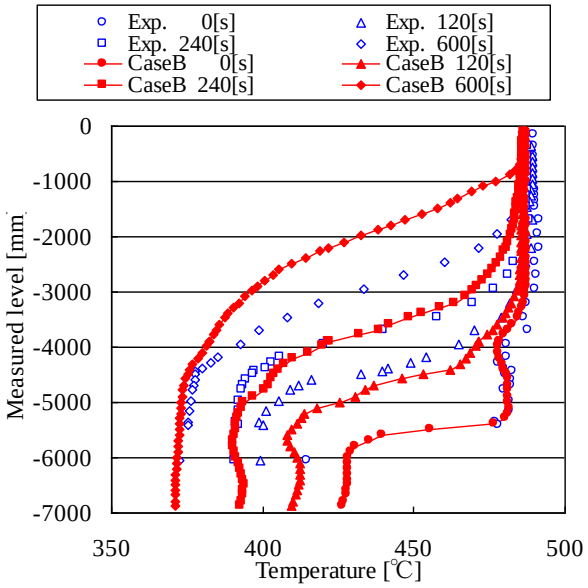

Fig. 12 Temperature distribution of the benchmark analyses

Figure 13 shows the analytical results of a) temperature distribution and b) velocity. At the initial condition, the high temperature flow from the core outlet goes upward and collides with the UCS. Then it flows obliquely upward as shown in Fig. 13b) (0s). As a result, no horizontal stratification interface is investigated as seen in Fig. 13a).

After the trip sequence is conducted, the cold sodium from the core outlet spreads horizontally because the hot sodium acts as a plug due to buoyancy. Consequently, the interface of the thermal stratification develops horizontally as in Fig. 13a). In the present analysis, almost no oscillation of the interface is investigated in the circumferential direction during the analysis.

In the analysis, no obvious change of the flow pattern is investigated during 120s-600s. Therefore, the interface of the stratification goes upwards almost constantly as seen in Figs. 12 and 13a). On the other hand, the growth of the interface in the vertical direction was suppressed during 240s-600s in the test as seen in

Fig. 12. In other words, it can be said that the plugging effect by the hot sodium was not weaken in the test during that period.

For instance, the upper plenum has the inner structure such as the UCS. As seen in Fig 13a), the UCS faces to the hot sodium and the temperature of the UCS would be enough high to transfer the heat towards the hot sodium at the beginning of the transient. From the viewpoint of the plugging effect by the hot sodium, it might be said that the heat capacity of the UCS is not negligible especially at the early stage of the transient.

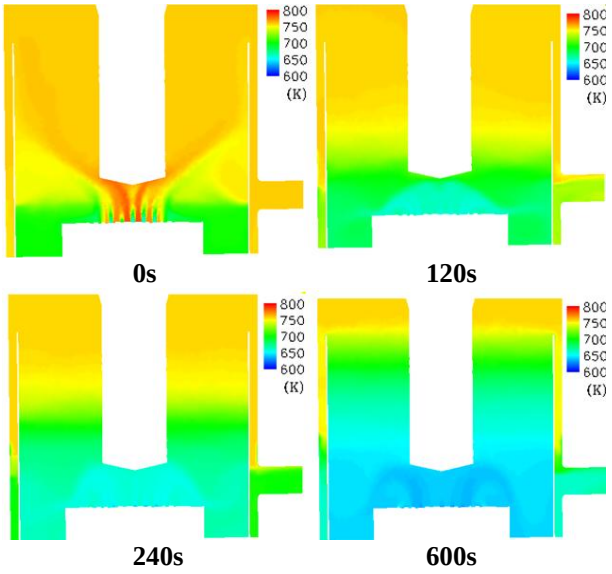

(a) Temperature distribution

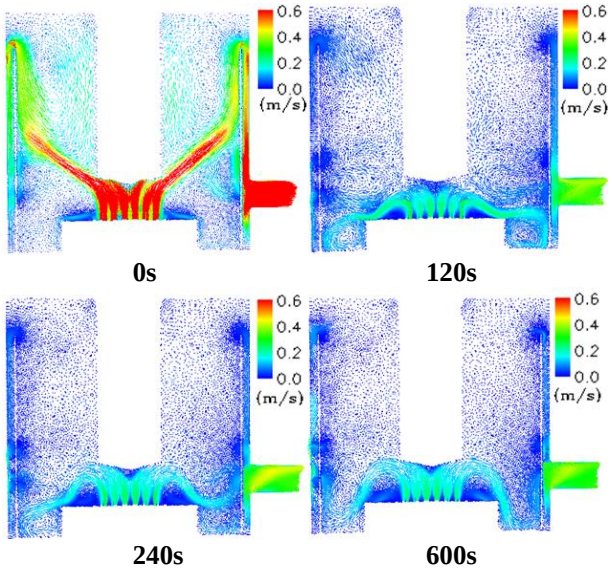

(b) Stream regime

Fig. 13 Vertical cross-sectional view of temperature distribution (a) and stream regime (b)

It is also mentioned that the elevation of the free surface of liquid sodium at the upper plenum would come down as the average sodium temperature decreases resulting in the change of the flow resistance of the overflow through the inner barrel. The numerical investigation of the influence of the free surface elevation will be planned in the future work.

4. CONCLUSION

Multi-dimensional numerical analyses of the turbine trip test of Monju from 40% power output condition have been carried out in the present study to investigate the characteristics of thermal stratification phenomena.

In the parametric study, a simplified analytical condition is applied in order to select the computational condition for the benchmark analysis. As a result, the certain numerical condition, such as the mesh arrangement at the flow halls and the time step size, are determined.

In the benchmark analysis of the turbine trip test, it is demonstrated that a good agreement is achieved at an early stage of the transient (0-240s). It can be concluded that the present numerical simulation is applicable to investigate the thermal stratification phenomena.

At the same time, it is also demonstrated that the elevation of the interface of the thermal stratification is overestimated after 240s from the trip in the analysis comparing with the test result. In the analysis, the flow pattern of the cold sodium from the core outlet seems to have not a big difference regardless of the transient during 120-600s resulting in almost the constant rise of the elevation.

On the contrary, the elevation of the interface seemed to be suppressed in the test at that period. It will be said that the heat capacity of the upper core structure (UCS) and the depth between the free surface of liquid sodium and the top of the inner barrel may influence the plugging effect.

A parametric study of, such as the heat capacity and the depth, will be planned in the future work in order to understand the stratification phenomena in the trip test.

REFERENCES

ANSYS, Inc., "http://www.ansys.com/products/fluid-dynamics/fluent/"

Doi, Y. *et al.* (1996). "Thermal Stratification Tests in Monju Upper plenum (1) –Temperature Distributions under Normal and Scram Condition with 40% power operation-" May 1996

Doi, Y. *et al.* (1997). "Investigation of Analytical Methods in Thermal Stratification analysis –Evaluation of flow rates through holes for normal and scram conditions of 40% power operation with AQUA code-" PNC TN9410 97-083

Ieda, Y. *et al.* (1990). "Experimental and Analytical Studies of The Thermal Stratification Phenomenon in The Outlet Plenum of Fast Breeder Reactors," Nuclear Engineering and Design 120, pp.403-414.

Maekawa, I. (1990), "Numerical Diffusion in Single-phase Multi-dimensional Thermal-hydraulic Analysis," Nuclear Engineering and Design 120, P323-339.

Ohno, S. *et al.* (2009). "Numerical Analysis of Sodium

Experiment for Thermal Stratification in Upper Plenum of Fast Reactor" , NURETH-13 Kanazawa City, Ishikawa Prefecture, Japan, September 27-October 2, 2009.

Suda, K. *et al.* (2002). "Numerical Analysis of Thermal Stratification Phenomena in Upper Plenum of a Fast Breeder Reactor (1) -Evaluation of thermal stratification phenomena near the region of flow holes-"

Yoshikawa, S. *et al.* (2009). "Data Description for Coordinated Research Project on Benchmark Analyses of Sodium Natural Convection in the Upper Plenum of the MUNJU Reactor Vessel", JAEA-Data/Code, 2008-024